



OPEN

Many-body and temperature effects in two-dimensional quantum droplets in Bose–Bose mixtures

Abdelâali Boudjemâa

We study the equilibrium properties of self-bound droplets in two-dimensional Bose mixtures employing the time-dependent Hartree–Fock–Bogoliubov theory. This theory allows one to understand both the many-body and temperature effects beyond the Lee–Huang–Yang description. We calculate higher-order corrections to the excitations, the sound velocity, and the energy of the droplet. Our results for the ground-state energy are compared with the diffusion Monte Carlo data and good agreement is found. The behavior of the depletion and anomalous density of the droplet is also discussed. At finite temperature, we show that the droplet emerges at temperatures well below the Berezinskii–Kosterlitz–Thouless transition temperature. The critical temperature strongly depends on the interspecies interactions. Our study is extended to the finite size droplet by numerically solving the generalized finite-temperature Gross–Pitaevskii equation which is obtained self-consistently from our formalism in the framework of the local density approximation.

Recently, the investigation of self-bound droplet states in Bose mixtures^{1–5} and dipolar ultracold gases^{6–8} has become a burgeoning area of interest. This novel state of matter forms due to the intriguing competition between the attractive mean-field interactions and the repulsive force furnished by the Lee–Huang–Yang (LHY) quantum fluctuations. The most important feature of these peculiar breakthroughs is that they are ultradilute contrary to the liquid Helium droplets⁹. Quantum droplets have been extensively researched in various contexts (see for review^{10–12} and references therein).

The binary Bose–Einstein condensates (BECs) with weak attractive inter- and repulsive intraspecies interactions support also the creation of ultradilute liquid-like droplets in two-dimensional (2D) configuration¹³. In the last few years, 2D quantum droplets have been studied from a variety of aspects including: effects of the spin-orbit coupling¹⁴, formation and stability of quantum Rabi-coupled droplets¹⁵, superfluidity and vortices¹⁶, supersolid stripe phase¹⁷, dynamical excitations¹⁸, bulk properties and quantum phases^{19, 20}.

In previous studies, the most commonly employed theoretical tool for describing the static and the dynamics of the droplet is the generalized Gross–Pitaevskii equation (GPE). Although this model which is based on the Petrov's theory¹³ gives reasonable results, it suffers from different handicaps. First, the generalized GPE disagrees with some experimental measurements² and quantum Monte Carlo (QMC) method^{21, 22}. In addition, it fails to properly predict the critical atom number^{20, 23} and to describe effects of quantum correlations²³. In this regard, many theoretical works beyond the generalized GPE have been introduced to study the properties of self-bound droplets^{19–22, 24–28}. Among them, the pairing theory¹⁹ which has been used in order to improve the Petrov's theory¹³ for quantum droplets of 2D Bose mixtures. However, the pairing approach gives almost the same results as the Petrov's theory for the ground-state energy. Both theories diverge from the diffusion Monte Carlo (DMC) simulation notably in the regime of small interspecies attraction. This discrepancy can be attributed to the absence of higher-order corrections that are crucial in 2D Bose systems.

Very recently, we have developed an interesting theoretical model beyond the standard LHY^{23, 29–31} called the time-dependent Hartree–Fock–Bogoliubov theory (TDHFB) able to self-consistently explain the behavior of quantum self-bound droplets at both zero and finite temperatures^{23, 29–31}. An essential feature of the variational TDHFB theory is that it takes into account the normal and anomalous fluctuations which are crucial, in order to have a consistent description of the droplet. Remarkably, in 3D our theory shows an excellent agreement with

¹Department of Physics, Faculty of Exact Sciences and Informatics, Hassiba Benbouali University of Chlef, P.O. Box 78, 02000 Ouled-Fares, Chlef, Algeria. ²Laboratory of Mechanics and Energy, Hassiba Benbouali University of Chlef, P.O. Box 78, 02000 Ouled-Fares, Chlef, Algeria. email: a.boudjemaa@univ-chlef.dz

DMC data and the previous theoretical results for the energy and the equilibrium density³¹. Regarding self-bound droplets of single dipolar BECs, the TDHFB provides also satisfactory explanations to experimental results and gives best match with the latest QMC simulation²³.

In this paper, we investigate many-body effects and impacts of higher-order quantum fluctuations on the ground-state properties of self-bound droplets of 2D symmetric Bose mixtures at both zero and finite temperatures using our HFB theory. At finite temperature this exotic states of matter remains largely unexplored most likely due to the self-evaporation i.e. non existence of collective excitations below the particle-emission threshold¹. We calculate analytically the contribution to the sound velocity, the ground-state energy and the free energy from higher-order quantum and thermal fluctuations. At zero temperature, the energy has a minimum at a finite density corresponding to a self-bound liquid-like droplet state. The obtained ground-state energy shows an excellent concordance with the DMC results of Ref. ¹³, indicating the relevance of our model. We analyze also the behavior of the depletion and the anomalous correlations of the droplet in terms of the equilibrium density. At finite temperature, we find that the self-bound droplet may occur only at a certain critical temperature well below the Berezinskii–Kosterlitz–Thouless (BKT) transition due to the crucial role played by thermal fluctuations effects. Such a critical temperature decreases as the strength of interspecies interactions grows. Furthermore, we show that our formalism provides an extended finite-temperature GPE in which higher-order logarithmic factors are added to the nonlinear term of the condensate. We use this model and discuss in particular the role of the quantum fluctuations play in the density profiles and the width of the droplet. To the best of our knowledge this is the first theoretical investigation of 2D self-bound Bose mixtures at finite temperature in the presence of higher-order corrections.

Results

Fluctuations and thermodynamics of 2D Bose mixtures

We consider a weakly interacting 2D Bose mixture with equal masses. The dynamics of this system including the effect of quantum and thermal fluctuations is governed by the coupled TDHDB equations which can be written in compact form as^{29–32}:

$$i\hbar \frac{d\Phi_j}{dt} = \left(h_j^{sp} + g_j n_j + g_{12} n_{3-j} + \delta\mu_{j\text{LHY}} \right) \Phi_j, \quad (1a)$$

$$i\hbar \frac{d\rho_j}{dt} = -2 \left[\rho_j, \frac{d\mathcal{E}}{d\rho_j} \right], \quad (1b)$$

where $\rho_j(\mathbf{r}, t)$ is the single particle density matrix of a thermal component defined as

$$\rho_j = \begin{pmatrix} \langle \hat{\psi}^\dagger \hat{\psi} \rangle & - \langle \hat{\psi} \hat{\psi} \rangle \\ \langle \hat{\psi}^\dagger \hat{\psi}^\dagger \rangle & - \langle \hat{\psi} \hat{\psi}^\dagger \rangle \end{pmatrix}_j,$$

and $\mathcal{E} = \sum_{j=1}^2 \left[\int d\mathbf{r} \left(\Phi_j^* h_j^{sp} \Phi_j + \hat{\psi}_j^\dagger h_j^{sp} \hat{\psi}_j + g_j n_j^2 / 2 \right) \right] + g_{12} \int d\mathbf{r} n_1 n_2 + \mathcal{E}_{\text{LHY}}$, is the energy of the system with $\mathcal{E}_{\text{LHY}} = \sum_{j=1}^2 (g_j/2) \int d\mathbf{r} (2\tilde{n}_j n_j - \tilde{n}_j^2 + |\tilde{m}_j|^2 + \tilde{m}_j^* \Phi_j^2 + \tilde{m}_j \Phi_j^{*2})$ being the LHY correction to the energy. In Eqs.(1) $h_j^{sp} = -(\hbar^2/2m_j)\Delta - \mu_j$ is the single particle Hamiltonian, μ_j is the chemical potential of each component, $\delta\mu_{j\text{LHY}}(\mathbf{r})\Phi_j(\mathbf{r}) = g_j [\tilde{n}_j(\mathbf{r})\Phi_j(\mathbf{r}) + \tilde{m}_j(\mathbf{r})\Phi_j^*(\mathbf{r})]$ is the relevant LHY term which is obtained self-consistently, $\hat{\psi}_j(\mathbf{r}) = \hat{\psi}(\mathbf{r}) - \Phi_j(\mathbf{r})$ is the noncondensed part of the field operator with $\Phi_j(\mathbf{r}) = \langle \hat{\psi}_j(\mathbf{r}) \rangle$, $n_{cj} = |\Phi_j|^2$ is the condensed density, $\tilde{n}_j = \langle \hat{\psi}_j^\dagger \hat{\psi}_j \rangle$ is the noncondensed density, $\tilde{m}_j = \langle \hat{\psi}_j \hat{\psi}_j \rangle$ is the anomalous correlation, and $n_j = n_{cj} + \tilde{n}_j$ is the total density of each species. In 2D Bose gases, the intra- and interspecies coupling strengths are given by $g_j = 4\pi\hbar^2 / [m \ln(4e^{-2\gamma}/a_j^2\kappa^2)]$ and $g_{12} = g_{21} = 4\pi\hbar^2 / [m \ln(4^2 e^{-2\gamma}/a_{12}^2\kappa^2)]$, where a_j and a_{12} being the 2D scattering lengths among the particles (see, e.g.,^{13, 33, 34}), $\gamma = 0.5772$ is Euler's constant. An adequate value of the cutoff κ can be obtained in the weakly interacting regime. In such a case, attraction (repulsion) can be reached when the scattering lengths are exponentially large (small) compared to the mean interparticle separation¹³.

The presence of the noncondensed and anomalous densities in Eq. (1) enables us to derive higher-order quantum corrections without any ad-hoc assumptions in contrast to the standard GPE. In our formalism \tilde{n}_j and \tilde{m}_j are related with each other via

$$I_j = (2\tilde{n}_j + 1)^2 - 4|\tilde{m}_j|^2. \quad (2)$$

This equation which stems from the conservation of the Von Neumann entropy, represents the variance of the number of noncondensed particles^{34, 35}. Equation (2) clearly shows that the anomalous density is not negligible even at zero temperature ($I \rightarrow 1$), contrary to what has been argued in the literature. Hence, \tilde{m} is crucial for the stability of Bose gases. Its involvement in such systems leads to a double counting of the interaction effects³⁰.

In order to calculate the elementary excitations and fluctuations of a homogeneous Bose mixture, we linearize Eqs. (1) using the generalized random-phase approximation (RPA): $\Phi_j = \sqrt{n_{cj}} + \delta\Phi_j$, $\tilde{n}_j = \tilde{n}_j + \delta\tilde{n}_j$, and $\tilde{m}_j = \tilde{m}_j + \delta\tilde{m}_j$, where $\delta\Phi_j(\mathbf{r}, t) = u_{jk} e^{i\mathbf{k}\cdot\mathbf{r} - i\epsilon_k t/\hbar} + v_{jk} e^{i\mathbf{k}\cdot\mathbf{r} + i\epsilon_k t/\hbar} \ll \sqrt{n_{cj}}$, $\delta\tilde{n}_j \ll \tilde{n}_j$, and $\delta\tilde{m}_j \ll \tilde{m}_j$ ^{29, 30}. Since

we restrict ourselves to second-order in the coupling constants, we keep only the terms which describe the coupling to the condensate and neglect all terms associated with fluctuations $\delta\tilde{n}_j$ and $\delta\tilde{m}_j$ (see Methods). The obtained second-order coupled TDHFB-de Gennes equations which are similar to the Beliaev's equations^{27, 36, 37}, provide correction terms to the Bogoliubov formula for the energy spectrum: $\varepsilon_{k\pm} = \sqrt{E_k^2 + 2E_k\mu_{\pm}}$ ³⁰, where $\mu_{\pm} = \bar{g}_1 n_{c1} [1 + \alpha \pm \sqrt{(1 - \alpha)^2 + 4\Delta^{-1}\alpha}]/2$, $\Delta = \bar{g}_1 \bar{g}_2 / g_{12}^2$, and $\alpha = \bar{g}_2 n_{c2} / \bar{g}_1 n_{c1}$. Here the density-dependent coupling constants $\bar{g}_j = g_j(1 + \tilde{m}_j/n_{cj})$ have been introduced in order to reinstate the gaplessness of the spectrum³⁰.

The noncondensed and anomalous densities can be computed through Eq. (2)^{30, 31}

$$\tilde{n}_{\pm} = \frac{1}{2} \int \frac{d\mathbf{k}}{(2\pi)^2} \left[\frac{E_k + \mu_{\pm}}{\varepsilon_{k\pm}} \sqrt{I_{k\pm}} - 1 \right], \quad (3)$$

and

$$\tilde{m}_{\pm} = -\frac{1}{2} \int \frac{d\mathbf{k}}{(2\pi)^2} \frac{\mu_{\pm}}{\varepsilon_{k\pm}} \sqrt{I_{k\pm}}, \quad (4)$$

where $I_{k\pm} = \coth^2(\varepsilon_{k\pm}/2T)$ ^{30, 31}.

At $T = 0$, integral (3) gives the following expression for the total depletion $\tilde{n} = \tilde{n}_+ + \tilde{n}_-$:

$$\tilde{n} = \frac{m^2}{4\pi\hbar^2} \sum_{\pm} c_{s\pm}^2, \quad (5)$$

where $c_{s\pm}^2 = \mu_{\pm}/m$ are the sound velocities which can be evaluated selfconsistently.

The integral in Eq. (4) is ultraviolet divergent and necessitates to be regularized^{34, 38, 39}. We use the dimensional regularization that is asymptotically accurate for weak interactions^{34, 40}. Then one analytically continues the result to finite coupling including a low-energy cutoff $\epsilon_c = \hbar^2\kappa^2/m \gg \mu_{\pm}$ ^{34, 38, 39}. This yields for the total anomalous density $\tilde{m} = \tilde{m}_+ + \tilde{m}_-$:

$$\tilde{m} = \frac{m^2}{4\pi\hbar^2} \sum_{\pm} c_{s\pm}^2 \ln\left(\frac{mc_{s\pm}^2}{\epsilon_c}\right), \quad (6)$$

For $g_{12} = 0$, Eqs. (5) and (6) recover those obtained by our second-order TDHFB-de Gennes equations³⁴ for a single component condensate.

The knowledge of the noncondensed and anomalous densities allows one to predict higher-order corrections to the free energy. In the frame of our formalism, it can be written as:

$$F = E + T \int \frac{d\mathbf{k}}{(2\pi)^2} \ln\left(\frac{2}{\sqrt{I_{k\pm}} + 1}\right), \quad (7)$$

where

$$E = E_0 + \frac{1}{2} \sum_{\pm} \int \frac{d\mathbf{k}}{(2\pi)^2} (\varepsilon_{k\pm} - E_k - \mu_{\pm}), \quad (8)$$

is the ground-state energy, and $E_0 = \frac{1}{2} \sum_{j=1}^2 g_j(n_{cj}^2 + 4n_{cj}\tilde{n}_j + 2\tilde{n}_j^2 + \tilde{m}_j^2 + 2n_{cj}\tilde{m}_j) + g_{12}n_1n_2$. The second term in Eq. (8) accounts for the LHY quantum corrections. It can be computed using the above dimensional regularization where only the bound modes that have energy lower than the magnitude of the binding energy are included in the integral¹⁹. The subleading term in Eq. (7) which represents the thermal effects is finite. Gathering quantum and thermal fluctuations contributions to the free energy (7), we get

$$F = E_0 + \frac{m^3}{8\pi\hbar^2} \sum_{\pm} c_{s\pm}^4 \ln\left(\frac{\sqrt{\epsilon} mc_{s\pm}^2}{\epsilon_c}\right) - \sum_{\pm} \frac{\zeta(3)}{(\hbar c_{s\pm})^2} T^3, \quad (9)$$

here we employed the identity $\int_0^{\infty} dx x \ln[2/(\coth(x/2) + 1)] = -\zeta(3)$, where $\zeta(3)$ is the Riemann zeta function. Expression (9) extends naturally the results of Petrov and Astrakharchik¹³ since it takes into account both many-body and temperature effects.

It is worth stressing that Eqs. (3)–(9) are self-consistent and must be solved iteratively.

Self-bound droplets

Now, we consider 2D symmetric Bose mixture with repulsive intraspecies interaction and attractive interspecies interaction where $a_{12}^{-1} \ll \sqrt{n} \ll a^{-1}$. The atoms are chosen to have equal intra-component scattering lengths $a_1 = a_2 = a$ and equal atom densities $n_1 = n_2 = n$, $\tilde{n}_1 = \tilde{n}_2 = \tilde{n}$, and $\tilde{m}_1 = \tilde{m}_2 = \tilde{m}$. For the sake of simplicity we put $\hbar = m = 1$.

Zero-temperature case. At zero temperature, the properties of self-bound ultradilute Bose mixtures can be analyzed by minimizing the ground-state energy with respect to the density or equivalently using the zero-pressure condition $P = \mu n - E/S = 0$, where S is the surface area¹³. According to the method outlined in Ref.¹³, we introduce a new set of coupling constants given as: $g = 4\pi/\ln(4e^{-2\gamma}/a^2\epsilon_0)$ and $g_{12} = 4\pi/\ln(4e^{-2\gamma}/a_{12}^2\epsilon_0)$,

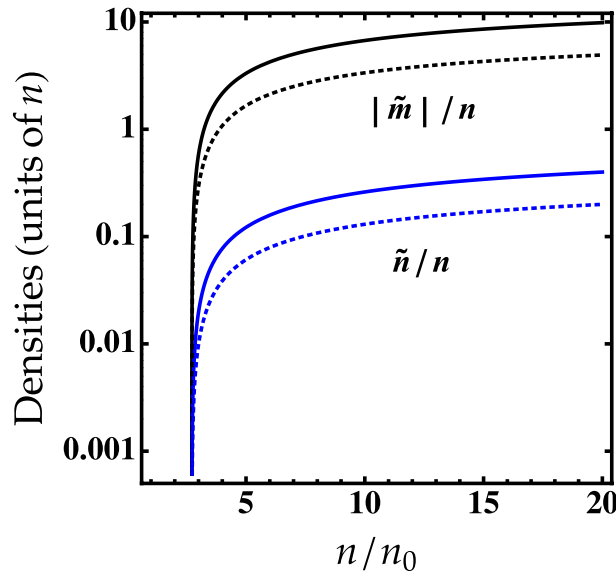


Figure 1. Noncondensed (11) and anomalous (12) fractions at the equilibrium as a function of n/n_0 for different values of $\ln(a_{12}/a)$. Solid lines: $\ln(a_{12}/a) = 5$. Dotted lines: $\ln(a_{12}/a) = 10$.

where $\epsilon_0 = 4e^{-2\gamma}/a_{12}a$ has been chosen in such a way that the condition $g^2 = g_{12}^2$ must be fulfilled. This implies that $c_{s-} = 0$ which means that $\tilde{n}_- = \tilde{m}_- = 0$. Then, the corrected sound velocity can be obtained via $c_s^2 = 2gn(1 - \tilde{n}/2n + \tilde{m}/2n)$ (here we set $c_{s+} = c_s$, $\tilde{n}_+ = \tilde{n}$, and $\tilde{m}_+ = \tilde{m}$ for convenience). For the purpose of analytical tractability, we keep only lowest order in \tilde{n} and \tilde{m} . This gives:

$$\frac{c_s^2}{c_{s0}^2} = \frac{1}{4\pi} \left(\frac{n}{n_0}\right) \left[\ln\left(\frac{n}{n_0}\right) - 1 \right], \tag{10}$$

where $n_0 = \epsilon_c/(2ge^{8\pi})$ is the equilibrium density which can be obtained by minimizing the ground-state energy (9) with respect to the density. The sound velocity at the equilibrium is defined as $c_{s0}^2 = gn_0$. Clearly, Eq. (10) predicts an imaginary sound velocity which may lead to a complex energy functional. Similar behavior has been reported in^{22,27} for 3D droplets. In the Petrov’s work^{1,13}, such a dynamically unstable phonon mode has been completely ignored under the assumption that its contribution is negligibly small. To stabilize the sound velocity and obtain the associated ground-state energy, we should include higher-order fluctuations (see below).

The noncondensed and anomalous densities of the droplet corresponding to the sound velocity (10) read:

$$\frac{\tilde{n}_{\text{eq}}}{n} = \frac{\ln(n/n_0) - 1}{\ln(a_{12}/a)}, \tag{11}$$

and

$$\frac{\tilde{m}_{\text{eq}}}{n} = \frac{\tilde{n}}{n} \ln \left[\frac{n/n_0(\ln(n/n_0) - 1)}{8\pi e^{8\pi}} \right], \tag{12}$$

Figure 1 shows that \tilde{m} is larger than \tilde{n} regardless of the value of $\ln(a_{12}/a)$ as in the case of self-bound droplets in 3D Bose mixtures³¹. Both densities are increasing with decreasing $\ln(a_{12}/a)$.

Let us now calculate the ground-state energy for 2D symmetric Bose mixtures by seeking the effect of higher-order fluctuations where a numerical method is used to treat the involved integration. The results are depicted in Fig. 2.

We see from Fig. 2a that the variation of the energy-cutoff which depends on interspecies interactions may strongly change the position of the local minimum of the energy leading to affect the stability and the existence of the droplet. For instance, for $\epsilon_0 \leq 0.1$, the local minimum disappears and the energy becomes positive indicating that the droplet may turn into a soliton-like many-body bound state in good agreement with the predictions of Refs.^{15,19,41}.

In Fig. 2b we compare our results for the ground-state energy up to second order in \tilde{m} and \tilde{n} of the iteration method with the DMC data and the Bogoliubov theory¹³. We see that when $\ln(a_{12}/a)$ gets larger, our results excellently agree with the DMC simulations and improve the standard Bogoliubov findings. This implies that for large $\ln(a_{12}/a)$, the HFB predictions become increasingly accurate due to the considerable role of higher-order terms arising from the normal and anomalous fluctuations. Our results diverge from the DMC simulations only for very small values of interspecies interaction $\ln(a_{12}/a) < 5$ and higher densities.

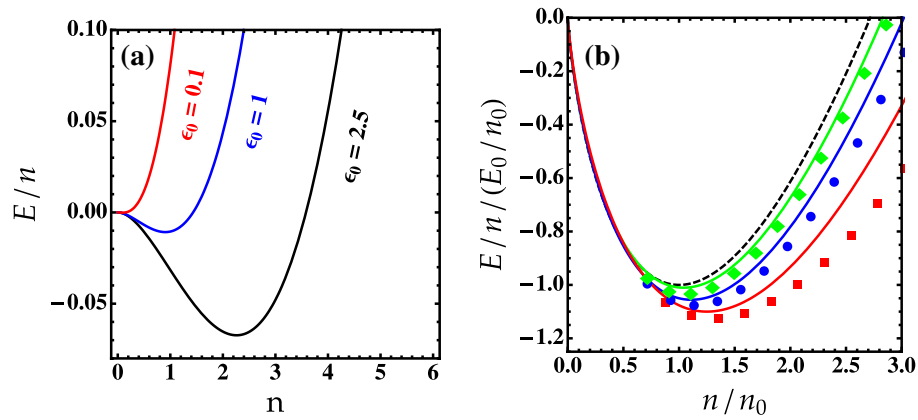


Figure 2. (a) The ground-state energy E/n from Eq. (8) for several values of ϵ_0 and $g = 0.45$. (b) The ground-state energy as a function of n/n_0 . Solid lines correspond to our beyond-LHY results up to second-order in \tilde{n} and \tilde{m} . Dashed line corresponds to the Bogoliubov theory¹³. Green diamonds ($\ln(a_{12}/a) = 20$), blue circles ($\ln(a_{12}/a) = 10$), and red squares ($\ln(a_{12}/a) = 5$) correspond to the DMC data of¹³. Here $E_0 = E(n_0)$.

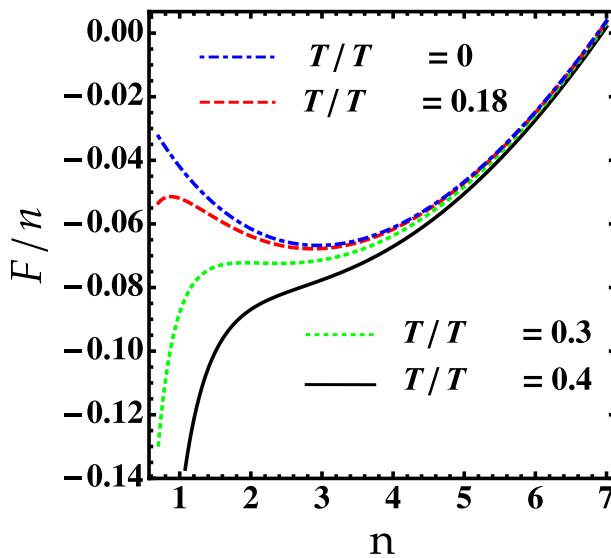


Figure 3. The free energy F/n as a function of the density for different values of temperature, T/T_{BKT} . Parameters are: $g = 0.45$, $g_{12} = 0.2$ and $\epsilon_0 = 4.8$.

Finite-temperature case. In homogeneous 2D Bose gases, thermal fluctuations are strong enough to prohibit the formation of a true BEC at any nonzero temperature^{42, 43}. However, according to BKT^{44, 45}, quasicondensate (or a condensate with only local phase coherence) takes place below the BKT transition temperature. The transition from a noncondensed state to quasicondensate occurs through the formation of bound vortex-antivortex pairs^{46, 47}. In such a quasicondensate, the phase coherence governs only regime of a size smaller than the size of the condensate, marked by the coherence length l_ϕ ⁴⁸. Therefore, below the BKT transition temperature one can use the HFB theory to describe the true BEC^{34, 49, 50} even though it cannot predict the critical fluctuations near the BKT region.

At finite temperature, the free energy becomes divergent since $c_{s-} = 0$ results in an unstable droplet in contrast to the zero-temperature case. Hence, to properly study the finite-temperature behavior of the 2D self-bound droplet, the sound velocity must be finite:

$$c_{s\pm}^2 = \delta g_{\pm} n \left[1 + \frac{\delta g_{\pm}}{4\pi} \ln \left(\frac{n \delta g_{\pm}}{\epsilon_c e} \right) \right], \tag{13}$$

where $\delta g_{\pm} = g \pm g_{12}$.

Minimizing the resulting free energy, we could observe the equilibrium emergence of the droplet, as visible in Fig. 3. The temperature is normalized to T_{BKT} which is defined for a symmetric mixture according to $T_{\text{BKT}} = \pi N \ln(380/g)/S$ ⁵⁰. It has been demonstrated that the interspecies interaction plays a minor role near the

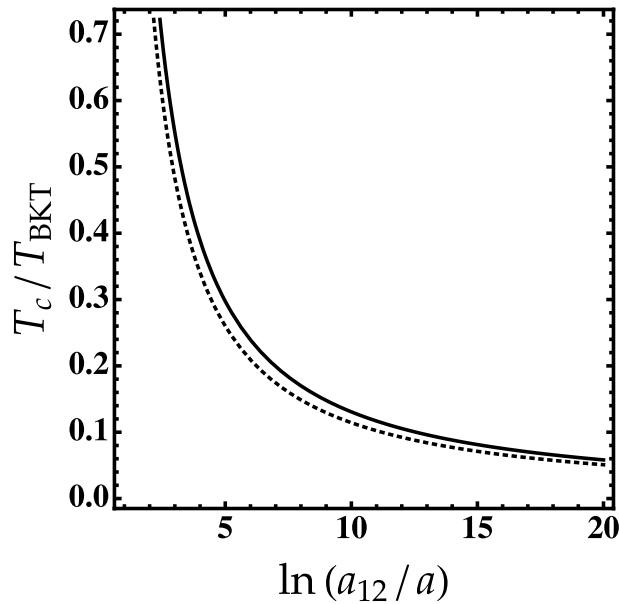


Figure 4. Critical temperature normalized to T_{BKT} as a function of $\ln(a_{12}/a)$. Solid line: without higher-order effects. Dotted line: higher-order effects.

BKT critical temperature^{51,52}. We see that the free energy F diverges like n^{-1} as the density goes to zero due to the presence of thermal fluctuations effects. Well below the BKT transition i.e. $0 < T \lesssim 0.3 T_{\text{BKT}}$, F develops a local maximum which corresponds to an unstable droplet, and a local minimum supporting a higher density stable self-bound solution. In such a regime, thermally excited atoms that occupy continuum modes are unbound and leave the droplet result in a process of self-cooling predicted earlier by Petrov¹. The two solutions disappear at the critical temperature ($T = T_c \simeq 0.3 T_{\text{BKT}}$) revealing that the liquid-like droplet start to evaporate. Increasing further the temperature ($T > T_c$), the free energy increases without any special structure and thus, the self-bound state loses its peculiar self-evaporation phenomenon and entirely destroys eventually. The same situation takes place for dipolar droplets in a single BEC^{53–55} and in dual condensates^{29,49}. Note that T_c strongly relies on ϵ_0 and hence, on the interspecies interactions as we shall see below.

The critical temperature above which the BEC-droplet phase transition occurs can be determined by minimizing the free energy. For $\delta g_- \ll \delta g_+$, one has

$$\frac{T_c}{T_{\text{BKT}}} \simeq \frac{\ln[(n/2e^{4\pi-2}n_0) - 1]^{1/3}}{(\pi\zeta(3))^{1/3} \ln(a_{12}/a) \ln[\ln(a_{12}/a)95/\pi]}, \tag{14}$$

As shown in Fig. 4 for fixed density n/n_0 , the droplet critical temperature decreases with the interspecies interaction $\ln(a_{12}/a)$ regardless the presence or not of the higher-order effects. For example for $\ln(a_{12}/a) = 20$, the droplet reaches its thermal equilibrium at ultralow temperature ($T_c \simeq 0.06 T_{\text{BKT}}$). We see also that higher-order corrections may reduce the critical temperature.

Generalized finite-temperature Gross–Pitaevskii equation

In this section, we consider the finite size effects on equilibrium properties of the self-bound droplet. The basic idea behind finite size contributions to the droplet’s energy is that the quantities Φ , \tilde{n} , and \tilde{m} must vary slowly at the scale of the extended healing length. As a consequence, we can include higher-order corrections locally as nonlinear terms in the TDHFB equations and treat them classically. For simplicity, we will ignore the dynamics of the thermal cloud and the anomalous correlations. Therefore, the TDHFB Eq. (1a) leads directly to the generalized finite-temperature GPE

$$i \frac{d\Phi}{dt} = -\frac{\nabla^2}{2} \Phi + \left[\frac{8\pi}{\ln^2(a_{12}/a)} \ln \left(\frac{|\Phi|^2}{\sqrt{\epsilon}n_0} \right) \alpha + \alpha_T \right] |\Phi|^2 \Phi, \tag{15}$$

where $\alpha \simeq \ln[(\epsilon n/n_0) \ln(n/\epsilon n_0)/8\pi e^{8\pi}]$, and $\alpha_T \simeq \zeta(3)T^3 \ln(a_{12}/a) / [2 \ln(|\Phi|^2/e^{4\pi+1}n_0) |\Phi|^4] [1/\ln(|\Phi|^2/e^{4\pi+1}n_0) + 1]$. Importantly, the generalized finite-temperature GPE (15) extends naturally the GPE of Ref.¹³ since it takes into account higher-order quantum and thermal corrections.

The stationary solutions of Eq. (15) can be found via the transformation $\Phi(\mathbf{r}, t) = \Phi(\mathbf{r}) \exp(-i\mu t)$. We solve the resulting static equation numerically using the split-step Fourier transform⁴. In Fig. 5, we plot the density profiles as a function of the radial distance at both zero and finite temperatures. As can be seen in Fig. 5a, the density n is flattened in accordance to the liquid character of the condensate. The obtained density is compared with the predictions of the GPE–LHY theory¹³. Our results show a slight deviation downwards for distance

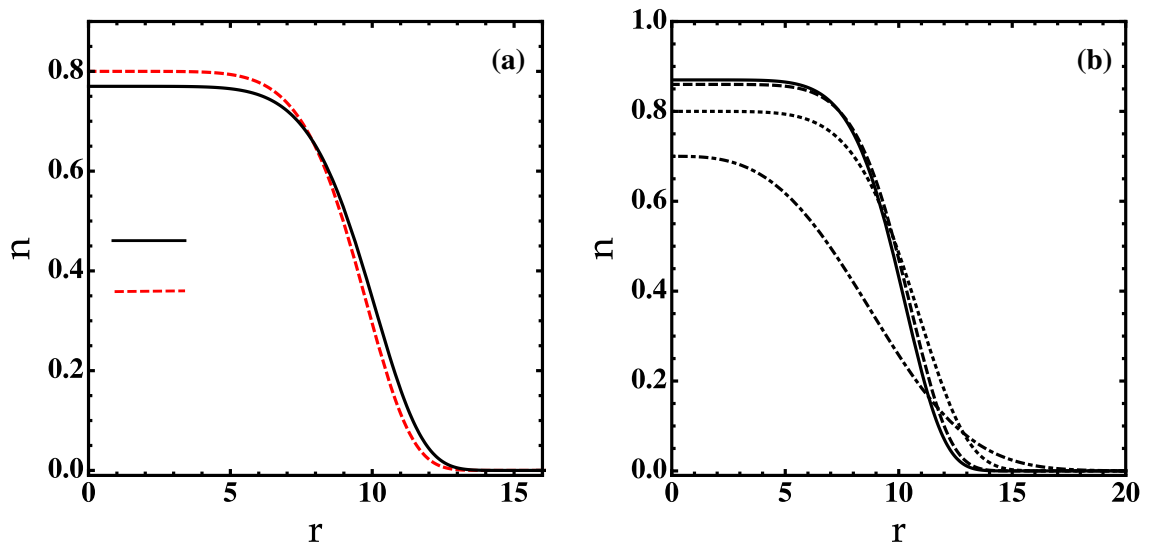


Figure 5. (a) Density profiles of the self-bound droplet obtained from the numerical solution of Eq. (15) at zero temperature for $N = 1000$ atoms and $\ln(a_{12}/a) = 20$. (b) Density profiles of the self-bound droplet obtained at different values of temperature for $N = 1000$ atoms and $\ln(a_{12}/a) = 20$. Solid line: $T = 0$. Dashed line: $T = 0.18T_{\text{BKT}}$. Dotted line: $T = 0.3T_{\text{BKT}}$. Dotted-Dashed line: $T = 0.4T_{\text{BKT}}$.

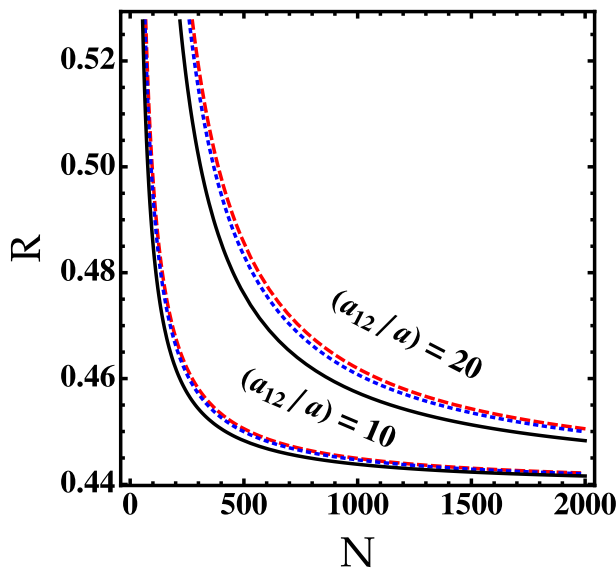


Figure 6. The self-bound droplet width as a function of the particles number N for different values of $\ln(a_{12}/a)$. The solid line corresponds to our generalized GPE (15). The red dashed line corresponds to the standard GPE¹³. The blue dotted line corresponds to the variational calculation.

$r < 8$ with respect to the findings of Ref.¹³ owing to the higher-order quantum fluctuations. At temperatures $T \lesssim T_c$, the droplet exhibits a weak-temperature dependence (see Fig.5b). Whereas, at $T \geq T_c$, the droplet has a Gaussian-like shape pointing out that the system experiences droplet-BEC phase transition.

To evaluate the width of the self-bound droplet, we first use the following trial wavefunction : $\Phi(r) = \exp(-r^2/2R^2)/\sqrt{\pi}R$, where R is the self-bound droplet width. Then, we minimize the resulting functional energy with respect to R . In the absence of the higher-order corrections, the width takes the form

$$R \simeq \frac{1}{\sqrt{\pi}} \exp [-(1/4) + \ln^2(a_{12}/a)/8N]. \tag{16}$$

This analytical prediction is reported in Fig. 6 and compared with the numerical results of our generalized GPE (15). We see that the width of the droplet decreases exponentially versus the number of particles. The interspecies interactions a_{12}/a lead also to reduce the width. The comparison between our predictions and those of Petrov¹³ indicates that the higher-order quantum effects may shift the droplet width. At finite temperature one

can expect that the droplet size increases significantly only at temperatures $T \gtrsim T_c$. Above such a temperature the self-bound droplet is in its thermal stabilization.

Discussion

We studied the equilibrium properties of symmetric self-bound droplets of 2D binary BEC beyond the standard LHY treatment, at both zero and finite temperatures. We computed higher-order corrections to the excitations spectrum, the sound velocity, the normal and anomalous correlations, and the free energy. These corrections improve the ground-state energy obtained from the Bogoliubov approach¹³ predicting an energy in good agreement with recent DMC simulations owing to the non-negligible role of higher order terms. At finite temperature, we revealed that the droplet occurs at temperature well below the BKT transition and destroys when the temperature becomes slightly larger than the ground-state energy of the droplet due to the thermal fluctuations effects. We found that the interspecies interaction tends to lower the critical temperature. We analyzed in addition the finite-size droplets in the framework of our generalized finite-temperature GPE. As outlined above, one can infer that in 2D mixtures, the droplet survives only in an ultradilute regime and at ultralow temperatures.

Our results could be extended in weakly interacting quasi-2D Bose mixtures as long as the following condition is fulfilled $0 < -a_{12}^{3D} < a^{3D} \ll l_0^{13}$, where a^{3D} and a_{12}^{3D} are the 3D intra and interspecies scattering lengths, and l_0 is the oscillator length in the confinement direction. The creation of such 2D mixture droplets in the experiment, still remains a challenging question.

Methods

Derivation of the condensate fluctuations. As we concluded in the main text, for a thermal distribution at equilibrium and by working in the momentum space, one has³⁴

$$\rho_{mn}(\mathbf{r} - \mathbf{r}') = \int \frac{d\mathbf{k}}{(2\pi)^3} e^{i\mathbf{k}\cdot(\mathbf{r}-\mathbf{r}')} \rho_{mn}(\mathbf{k}), \tag{17}$$

where $\rho_{mn}(\mathbf{k})$ is the Fourier transform of $\rho_{mn}(\mathbf{r} - \mathbf{r}')$. After some algebra, expression (2) turns out to be given as:

$$I_{k\pm} = (2\tilde{n}_{\pm k} + 1)^2 - |2\tilde{m}_{\pm k}|^2 = \coth^2(\varepsilon_{k\pm}/2T), \tag{18}$$

From Eq. (18) we can straightforwardly derive the expressions (3) and (4) describing the normal and anomalous correlations. For an ideal Bose gas where the anomalous density vanishes, $I_k = \coth^2(E_k/2T)$ ³⁰.

TDHFB-de Gennes equations. We use the generalized RPA which consists of imposing small fluctuations of the condensates, the noncondensates, and the anomalous components, respectively, as: $\Phi_j = \sqrt{n_{cj}} + \delta\Phi_j$, $\tilde{n}_j = \tilde{n}_j + \delta\tilde{n}_j$, and $\tilde{m}_j = \tilde{m}_j + \delta\tilde{m}_j$, where $\delta\Phi_j \ll \sqrt{n_{cj}}$, $\delta\tilde{n}_j \ll \tilde{n}_j$, and $\delta\tilde{m}_j \ll \tilde{m}_j$ ³⁰. We then obtain the TDHFB-RPA equations:

$$i\hbar\delta\dot{\Phi}_j = \left[h_j^{sp} + 2\bar{g}_j n_{cj} + 2g_j \tilde{n}_j + g_{12} n_{3-j} \right] \delta\Phi_j + \bar{g}_j n_{cj} \delta\Phi_j^* + 2g_j \sqrt{n_{cj}} \delta\tilde{n}_j + g_{12} \sqrt{n_{c3-j}} \delta\tilde{n}_{3-j} + g_{12} \sqrt{n_{cj} n_{c3-j}} (\delta\Phi_{3-j} + \delta\Phi_{3-j}^*), \tag{19}$$

and

$$i\hbar\delta\dot{\tilde{m}}_j = 4 \left[h_j^{sp} + 2g_j n_j + g_j \bar{g}_j / 4 (\bar{g}_j - g_j) (2\tilde{n}_j + 1) + g_{12} n_{3-j} \right] \delta\tilde{m}_j + 8g_j \tilde{m}_j \left[\sqrt{n_{cj}} (\delta\Phi_j + \delta\Phi_j^*) + \delta\tilde{n}_j + \bar{g}_j / 4 (\bar{g}_j - g_j) \delta\tilde{n}_j \right] + g_{12} \tilde{m}_j \left[\sqrt{n_{c3-j}} (\delta\Phi_{3-j} + \delta\Phi_{3-j}^*) + \delta\tilde{n}_{3-j} \right], \tag{20}$$

Remarkably, this set of equations contains a class of terms beyond second order. Note that we keep in Eqs. (19) and (20) only the terms which describe the coupling to the condensate and neglect all terms associated with $\delta\tilde{n}$ and $\delta\tilde{m}$ owing to the fact that we restrict ourselves to second-order in the coupling constants.

Inserting the transformation $\delta\Phi_j(\mathbf{r}, t) = u_{jk} e^{i\mathbf{k}\cdot\mathbf{r} - i\varepsilon_k t/\hbar} + v_{jk} e^{i\mathbf{k}\cdot\mathbf{r} + i\varepsilon_k t/\hbar}$ into Eq. (19), we find the second-order coupled TDHFB-de Gennes equations for the quasiparticle amplitudes u_{kj} and v_{kj} :

$$\begin{pmatrix} \mathcal{L}_1 & \mathcal{M}_1 & \mathcal{A} & \mathcal{A} \\ \mathcal{M}_1 & \mathcal{L}_1 & \mathcal{A} & \mathcal{A} \\ \mathcal{A} & \mathcal{A} & \mathcal{L}_2 & \mathcal{M}_2 \\ \mathcal{A} & \mathcal{A} & \mathcal{M}_2 & \mathcal{L}_2 \end{pmatrix} \begin{pmatrix} u_{1k} \\ v_{1k} \\ u_{2k} \\ v_{2k} \end{pmatrix} = \varepsilon_k \begin{pmatrix} u_{1k} \\ -v_{1k} \\ u_{2k} \\ -v_{2k} \end{pmatrix}, \tag{21}$$

where $\int d\mathbf{r} [u_j^2(\mathbf{r}) - v_j^2(\mathbf{r})] = 1$, $\mathcal{L}_j = E_k + 2\bar{g}_j n_{cj} + 2g_j \tilde{n}_j + g_{12} n_{3-j} - \mu_j$, $\mathcal{M}_j = \bar{g}_j n_{cj}$, and $\mathcal{A} = g_{12} \sqrt{n_{c1} n_{c2}}$. Equations (21) are appealing since they enable us to calculate in a simpler manner corrections to the excitations spectrum $\varepsilon_{k\pm}$ of homogeneous Bose mixtures (see the main text).

Received: 23 August 2021; Accepted: 15 October 2021

Published online: 05 November 2021

References

- Petrov, D. S. Quantum mechanical stabilization of a collapsing Bose–Bose mixture. *Phys. Rev. Lett.* **115**, 155302 (2015).
- Cabrera, C. R. *et al.* Quantum liquid droplets in a mixture of Bose–Einstein condensates. *Science* **359**, 301 (2018).
- Cheiney, P. *et al.* Bright soliton to quantum droplet transition in a mixture of Bose–Einstein condensates. *Phys. Rev. Lett.* **120**, 135301 (2018).
- Semeghini, G. *et al.* Self-bound quantum droplets of atomic mixtures in free space. *Phys. Rev. Lett.* **120**, 235301 (2018).
- D’Errico, C. *et al.* Observation of quantum droplets in a heteronuclear bosonic mixture. *Phys. Rev. Res.* **1**, 033155 (2019).
- Kadau, H. *et al.* Observing the Rosensweig instability of a quantum ferrofluid. *Nature* **530**, 194 (2016).
- Schmitt, M., Wenzel, M., Böttcher, F., Ferrier-Barbut, I. & Pfau, T. Self-bound droplets of a dilute magnetic quantum liquid. *Nature* **539**, 259 (2016).
- Chomaz, L. *et al.* Quantum-fluctuation-driven crossover from a dilute Bose–Einstein condensate to a macrodroplet in a dipolar quantum fluid. *Phys. Rev. X* **6**, 041039 (2016).
- Volovik, G. E. *The Universe in a Helium Droplet* (Oxford University Press, 2009).
- Luo, Z.-H., Pang, W., Liu, B., Li, Y.-Y. & Malomed, B. A. A new form of liquid matter: Quantum droplets. *Front. Phys.* **16**, 32201 (2021).
- Böttcher, F. *et al.* Pattern Formation in quantum ferrofluids: From supersolids to superglasses. *Rep. Prog. Phys.* **84**, 012403 (2021).
- Guo, M. & Pfau, T. A new state of matter of quantum droplets. *Front. Phys.* **16**, 32202 (2021).
- Petrov, D. S. & Astrakharchik, G. E. Ultradilute low-dimensional liquids. *Phys. Rev. Lett.* **117**, 100401 (2016).
- Li, Y. *et al.* Two-dimensional solitons and quantum droplets supported by competing self- and cross-interactions in spin-orbit-coupled condensates. *New J. Phys.* **19**, 113043 (2017).
- Chiquillo, E. Low-dimensional self-bound quantum Rabi-coupled bosonic droplets. *Phys. Rev. A* **99**, 051601(R) (2019).
- Li, Y. *et al.* Two-dimensional vortex quantum droplets. *Phys. Rev. A* **98**, 063602 (2018).
- Sachdeva, R., Tengstrand, M. N. & Reimann, S. M. Self-bound supersolid stripe phase in binary Bose–Einstein condensates. *Phys. Rev. A* **102**, 043304 (2020).
- Otajonov, S. R., Tsoy, E. N. & Abdullaev, FKh. Variational approximation for two-dimensional quantum droplets. *Phys. Rev. E* **102**, 062217 (2020).
- Hu, H., Wang, J. & Liu, X.-J. Microscopic pairing theory of a binary Bose mixture with interspecies attractions: Bosonic BEC-BCS crossover and ultradilute low-dimensional quantum droplets. *Phys. Rev. A* **102**, 043301 (2020).
- Pan, J., Yi, S., & Shi, T. Quantum phases of self-bound droplets of Bose–Bose mixtures. <http://arxiv.org/abs/2102.02361v1> (2021).
- Cikojevic, V., Markic, L. V., Astrakharchik, G. E. & Boronat, J. Universality in ultradilute liquid Bose–Bose mixtures. *Phys. Rev. A* **99**, 023618 (2019).
- Ota, M. & Astrakharchik, G. E. Beyond Lee–Huang–Yang description of self-bound Bose mixtures. *Sci. Post Phys.* **9**, 020 (2020).
- Boudjemâa, A. & Guebli, N. Quantum correlations in dipolar droplets: Time-dependent Hartree–Fock–Bogoliubov theory. *Phys. Rev. A* **102**, 023302 (2020).
- Cappellaro, A., Macri, T., Bertacco, G. F. & Salasnich, L. Equation of state and self-bound droplet in Rabi-coupled Bose mixtures. *Sci. Rep.* **7**, 13358 (2017).
- Staudinger, C., Mazzanti, F. & Zillich, R. E. Self-bound Bose mixtures. *Phys. Rev. A* **98**, 023633 (2018).
- Cappellaro, A., Macri, T. & Salasnich, L. Collective modes across the soliton-droplet crossover in binary Bose mixtures. *Phys. Rev. A* **97**, 053623 (2018).
- Gu, Q. & Yin, L. Phonon stability and sound velocity of quantum droplets in a Bose mixture. *Phys. Rev. B* **102**, 220503 (R) (2020).
- Cikojevic, V., Markic, L. V. & Boronat, J. Finite-range effects in ultradilute quantum drops. *New J. Phys.* **22**, 053045 (2020).
- Boudjemâa, A. Fluctuations and quantum self-bound droplets in a dipolar Bose–Bose mixture. *Phys. Rev. A* **98**, 033612 (2018).
- Boudjemâa, A. Quantum and thermal fluctuations in two-component Bose gases. *Phys. Rev. A* **97**, 033627 (2018).
- Guebli, N. & Boudjemâa, A. Quantum self-bound droplets in Bose–Bose mixtures: Effects of higher-order quantum and thermal fluctuations. *Phys. Rev. A* **104**, 023310 (2021).
- Boudjemâa, A. Self-localized state and solitons in a Bose–Einstein-condensate-impurity mixture at finite temperature. *Phys. Rev. A* **90**, 013628 (2014).
- Popov, V. N. Functional integrals in quantum field theory and statistical physics. *Theor. Math. Phys.* **11**, 565 (1983).
- Boudjemâa, A. Behavior of the anomalous correlation function in a uniform two-dimensional Bose gas. *Phys. Rev. A* **86**, 043608 (2012).
- Boudjemâa, A. & Benarous, M. On the anomalous density for Bose gases at finite temperature. *Phys. Rev. A* **84**, 043633 (2011).
- Beliaev, S. T. Application of quantum field theory methods to a system of Bose-particles. *Sov. Phys. JETP* **7**, 289 (1958).
- Beliaev, S. T. Energy spectrum of a non-ideal Bose gas. *Sov. Phys. JETP* **34**, 299 (1958).
- Andersen, J. O. Theory of the weakly interacting Bose gas. *Rev. Mod. Phys.* **76**, 599 (2004).
- Salasnich, L. & Toigo, F. Zero-point energy of ultracold atoms. *Phys. Rep.* **640**, 1 (2016).
- Yukalov, V. I. Basics of Bose–Einstein condensation. *Phys. Part. Nucl.* **42**, 460 (2011).
- Hammer, H.-W. & Son, D. T. Universal properties of two-dimensional boson droplets. *Phys. Rev. Lett.* **93**, 250408 (2004).
- Mermin, N. D. & Wagner, H. Absence of ferromagnetism or antiferromagnetism in one- or two-dimensional isotropic Heisenberg models. *Phys. Rev. Lett.* **22**, 1133 (1966).
- Hohenberg, P. C. Existence of long-range order in one and two dimensions. *Phys. Rev.* **158**, 383 (1967).
- Berezinskii, V. L. Destruction of long range order in one dimensional and two-dimensional systems having a continuous symmetry Group II. quantum systems. *Sov. Phys. JETP* **34**, 610 (1972).
- Kosterlitz, J. M. & Thouless, D. J. Ordering, metastability and phase transitions in two-dimensional systems. *J. Phys. C* **6**, 1181 (1973).
- Prokof’ev, N., Ruebenacker, O. & Svistunov, B. Critical point of a weakly interacting two-dimensional Bose gas. *Phys. Rev. Lett.* **87**, 270402 (2001).
- Chomaz, L. *et al.* Emergence of coherence via transverse condensation in a uniform quasitwo-dimensional Bose gas. *Nat. Commun.* **6**, 6172 (2015).
- Petrov, D. S., Gangardt, D. M. & Shlyapnikov, G. V. Low-dimensional trapped gases. *J. Phys. I* **116**, 5 (2004).
- Boudjemâa, A. & Shlyapnikov, G. V. Two-dimensional dipolar Bose gas with the Roton–Maxon excitation spectrum. *Phys. Rev. A* **87**, 025601 (2013).
- Roy, A., Ota, M., Recati, A. & Dalfovo, F. Finite-temperature spin dynamics of a two-dimensional Bose–Bose atomic mixture. *Phys. Rev. Res.* **3**, 013161 (2021).
- Karle, V., Defenu, N. & Enns, T. Coupled superfluidity of binary Bose mixtures in two dimensions. *Phys. Rev. A* **99**, 063627 (2019).
- Kobayashi, M., Eto, M. & Nitta, M. Berezinskii–Kosterlitz–Thouless transition of two-component Bose mixtures with intercomponent Josephson coupling. *Phys. Rev. Lett.* **123**, 075303 (2019).
- Boudjemâa, A. Quantum dilute droplets of dipolar bosons at finite temperature. *Ann. Phys.* **381**, 68 (2017).
- Boudjemâa, A. Two-dimensional quantum droplets in dipolar Bose gases. *New J. Phys.* **21**, 093027 (2019).
- Aybar, E. & Oktel, M. Ö. Temperature-dependent density profiles of dipolar droplets. *Phys. Rev. A* **99**, 013620 (2019).

Author contributions

The author conceived the work, obtained the results, wrote and reviewed the manuscript.

Competing interests

The author declares no competing interests.

Additional information

Correspondence and requests for materials should be addressed to A.B.

Reprints and permissions information is available at www.nature.com/reprints.

Publisher's note Springer Nature remains neutral with regard to jurisdictional claims in published maps and institutional affiliations.



Open Access This article is licensed under a Creative Commons Attribution 4.0 International License, which permits use, sharing, adaptation, distribution and reproduction in any medium or format, as long as you give appropriate credit to the original author(s) and the source, provide a link to the Creative Commons licence, and indicate if changes were made. The images or other third party material in this article are included in the article's Creative Commons licence, unless indicated otherwise in a credit line to the material. If material is not included in the article's Creative Commons licence and your intended use is not permitted by statutory regulation or exceeds the permitted use, you will need to obtain permission directly from the copyright holder. To view a copy of this licence, visit <http://creativecommons.org/licenses/by/4.0/>.

© The Author(s) 2021